

## Rayleigh scattering of two x-ray photons by an atom

Alexey N. Hopersky, Alexey M. Nadolinsky, and Sergey A. Novikov\*

*Chair of Mathematics, Rostov State Transport University, Rostov-on-Don 344038, Russia*

(Received 31 December 2015; published 4 May 2016)

The process of elastic (Rayleigh) scattering of two x-ray free-electron laser (XFEL) photons by a free He atom is theoretically investigated. We obtain the absolute values and the forms of the triple differential scattering cross section. The main theoretical result is the highest probability of creation of scattered photons with energy  $\hbar\omega_{\pm} \cong \hbar\omega \pm I_{1s}$  ( $\hbar\omega$  is the energy of the incident XFEL photon,  $I_{1s}$  is the energy of the ionization threshold of the  $1s^2$  atomic shell). The probability of creation cooled ( $<\omega_-$ ) and hot ( $>\omega_+$ ) photons is smaller by many orders of magnitude, and is identically zero when the formal (nonphysical) energy of one of the scattered photons is  $2\hbar\omega$ .

DOI: [10.1103/PhysRevA.93.052701](https://doi.org/10.1103/PhysRevA.93.052701)

### I. INTRODUCTION

The creation of x-ray free-electron laser (XFEL) (see Ref. [1] and references therein) provides an opportunity to investigate fundamental nonlinear processes at the microscopic scale. These processes, in particular, include elastic scattering of two x-ray photons by a free atom. This process occurs via creation of virtual excitation (ionization) states of the atom with consequent return to the original state. In that sense (creation of virtual atomic states) we retain the traditional (anomalous-dispersive elastic scattering of one photon by the atom) [2] name of Rayleigh scattering. The subject of our investigation is the atom of He (nuclear charge is  $Z = 2$ , configuration and ground-state term are  $[0] = 1s^2[1S_0]$ ), as it is the simplest element with a filled shell in the ground state. The choice for the He atom as the research subject was also due to the fact that He is affordable and is widely used in high-precision experiments (see, for example, Feldhaus *et al.* [1]).

### II. THEORY

Let us consider the process of Rayleigh scattering of two XFEL photons by He:

$$\omega + \omega + [0] \rightarrow X \rightarrow [0] + \omega_1 + \omega_2, \quad (1)$$

where  $\omega$  ( $\omega_{1,2}$ ) is the angular frequency of the incident (scattered) photon,  $X$  are the intermediate (virtual) scattering states and the conservation of energy has the form of  $\omega_1 + \omega_2 = 2\omega$ . In (1) and hereafter, we assume the atomic system of units:  $m_e = e = \hbar = 1$ , where  $m_e$  is the electron mass and  $e$  is the electron charge, and  $\hbar$  is Planck's constant. We restrict ourselves to the second order in the nonrelativistic quantum perturbation theory (as defined by the number of interaction vertices, Fig. 1). Then we can define four interfering probability amplitudes for process (1) over the scattering states:

$$\begin{cases} X_1 = 1sxl + \omega + \omega_2, & xl > F, \\ X_2 = 1sxl + \omega + \omega_1, \\ X_3 = 1sxl, \\ X_4 = 1sxl + \omega + \omega + \omega_1 + \omega_2. \end{cases} \quad (2)$$

Here,  $xl$  are the single electron excited (ionization) states of the  $1s^2$  shell, the orbital quantum number  $l \in [0; \infty)$ , and  $F$  is the Fermi level (set of quantum numbers of the  $1s^2$  shell of the atomic ground state).

The structure of scattering states (2) is defined by the form of the contact transition operator [3]:

$$\widehat{W} = \frac{1}{2c^2} \sum_{n=1}^N (\widehat{A}_n \cdot \widehat{A}_n), \quad (3)$$

where  $c$  is the speed of light in vacuum,  $\widehat{A}_n = \widehat{A}(0; \vec{r}_n)$  is the electromagnetic field operator in the second quantization picture at time  $t = 0$ ,  $\vec{r}_n$  is the radius vector of the  $n$ th electron, and  $N$  is the number of electrons in the atom. The notion of “contactness” of the interaction means that wave functions of two photons, electron, and vacancy converge in the same space-time point (Fig. 1).

Expansion of the number of intermediate scattering states investigated in (1) requires the transition to a third (and higher) order of the perturbation theory, and the consideration of the radiative transition operator [3,4]:

$$\widehat{V} = -\frac{1}{c} \sum_{n=1}^N (\widehat{p}_n \cdot \widehat{A}_n), \quad (4)$$

where  $\widehat{p}_n$  is the momentum operator of the  $n$ th electron. In this work we do not consider such an extension. The validity of this approach is due to two factors. First, an increase in the number of energy denominators suppressing partial scattering probability amplitudes. Second, the theoretical result of works [5] for bremsstrahlung probability amplitudes,  $m_{xy} = \langle xl | \widehat{p} | y(l \pm 1) \rangle \sim \delta(x - y)$ , where  $\delta$  is the Dirac  $\delta$  function. Indeed, for example, for the intermediate scattering  $xl$  and  $y(l \pm 1)$  states of the continuum, the scattering probability amplitudes of third (and higher) order of the perturbation theory, taking into account the structure of the free-free  $m_{xy}$  matrix element, are proportional to  $\delta(\omega) = \delta(\omega_{1,2}) = 0$  when  $\omega > 0$ ,  $\omega_{1,2} > 0$ . Thus, the amplitude of the third  $X = 1sx(s,d) + \omega + \omega_2 \rightarrow 1syp + \omega_2$  [Fig. 1(e)] and fourth  $X = 1sxp + \omega \rightarrow 1sy(s,d) \rightarrow 1szp + \omega_1$  [Fig. 1(f)] orders of the perturbation theory are proportional to  $\delta(\omega)$  and  $\delta(\omega)\delta(\omega_1)$ , respectively. For the intermediate scattering  $xl$  states of the discrete spectrum, scattering probability amplitudes of third

\*sanovikov@gmail.com

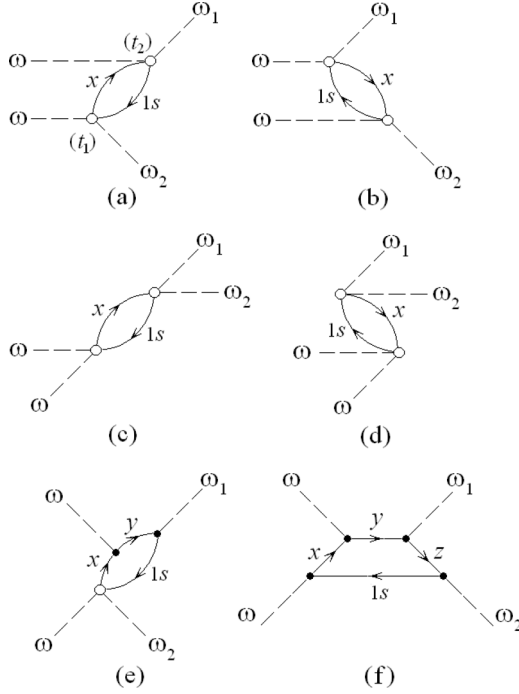


FIG. 1. Partial probability amplitudes for the Rayleigh scattering of two XFEL photons by a He atom in the Feynman diagram representation. Right arrow: electron ( $x \equiv xl > F$ ); left arrow: vacancy ( $1s$ ). Open circle: contact transition operator  $\widehat{W}$  interaction vertex. Solid circle: the vertex of interaction for the radiative transition operator  $\widehat{V}$ .  $\omega$  ( $\omega_{1,2}$ ) is the incident (scattered) photon. Time direction of the process is  $t_1 < t_2$ . (a, b, c, d, e, f); see Sec. II.

(and higher) perturbation theory orders contain a suppressing energy factor  $\sim \omega^{-1}$ .

In the second-order perturbation theory for the probability amplitude of process (1), operator (4) in the electromagnetic field interaction Hamiltonian atom is not taken into account [Figs. 1(a)–1(d)]. This leads to a violation of the requirement of local gauge invariance [3] for the scattering cross section (11) with respect to the  $\widehat{A}_\mu \rightarrow \widehat{A}_\mu - \partial\varphi/\partial x^\mu$  transformation of electromagnetic potential and initial (intermediate) atomic wave functions  $|\Psi\rangle \rightarrow \exp(i\varphi)|\Psi\rangle$ , where  $\varphi$  is an arbitrary function of space-time coordinates  $x^\mu = (ct; \vec{x})$ . To restore the local gauge invariance for the cross section (11), it is necessary to consider all orders of perturbation theory in the transition operators (3) and (4), as well as the complete set of atomic  $xl$  excitation and ionization states. Investigation of this problem is the subject of future research. Such studies, in particular, show a measure of violation (measure of the dependence on the choice of calibration of the electromagnetic field operator  $\widehat{A}_\mu$ ) of local gauge invariance for the cross section (11) when constrained by the fixed order of the nonrelativistic perturbation theory.

The physical interpretation of the probability amplitude for process (1) and states (2) in the Feynman diagram representation of nonrelativistic many-body quantum theory [4] is given in Fig. 1 and Sec. III of this paper. We restrict ourselves to the XFEL photon energies of  $2\omega \gg I_{1s}$ , where the ionization threshold energy of the  $1s^2$  shell of He is defined to be  $I_{1s} = 23.45$  eV (calculation of this work). Then, we can

neglect the probability amplitudes over states  $X_3$  [Fig. 1(c)] and  $X_4$  [Fig. 1(d)]. Indeed, for  $xl$  states of the continuum, for example, the probability amplitude singularity over state  $X_3$  is defined when  $x \cong 2\omega - I_{1s} \gg 0$ , whereas  $x \cong \omega - I_{1s} - \omega_{1,2} \rightarrow 0$  when  $\omega_{1,2} \rightarrow \omega - I_{1s}$  for the singularities over states  $X_{1,2}$ . In Sec. III we shall show that for scattered photons precisely in the energy range  $\omega_{1,2} \cong \omega \pm I_{1s}$ , giant maxima in the scattering spectra occur. The probability amplitude over state  $X_4$  is nonsingular and is suppressed by a large ( $\cong 2\omega + I_{1s} + x, x \geq 0$ ) energy denominator. Therefore, in the investigated range of energies for the XFEL photons, states  $X_1$  [Fig. 1(a)] and  $X_2$  [Fig. 1(b)] are the leading ones, and their total probability amplitude takes the form (see Appendix A):

$$\Phi = (\vec{e} \cdot \vec{e}_1)(\vec{e} \cdot \vec{e}_2) \left( \frac{\pi}{V} \right)^2 \frac{1}{\omega \sqrt{2\omega_1\omega_2}} D, \quad (5)$$

$$D = \sum_{x>F} Q \left( \frac{1}{\eta_1} + \frac{1}{\eta_2} \right), \quad (6)$$

$$Q = (4l + 2) R_l^{(1)} R_l^{(2)} P_l(\cos \Psi). \quad (7)$$

Here, function  $Q$  is derived through methods of the irreducible tensor operator theory (see Appendix B). We define the following:  $V$  is the quantization volume of the electromagnetic field,  $\sum_{x>F}$  is the symbol of summation over the discrete spectrum states [ $x > F \rightarrow nl > F$ ] and summation (integration) over the states of the continuous spectrum [ $\sum_{l=0}^{\infty} \int_0^{\infty} dx$ ],  $\eta_m = \omega - \omega_m - E(1sxl) + E(0)$ ,  $m = 1, 2$ ,  $\vec{e}$  ( $\vec{e}_m$ ) is the polarization vector of the incident (scattered) photon,  $E$  is the total Hartree-Fock energies of atomic states,  $R_l^{(m)} = \langle 1s | j_l(q_m r) | xl \rangle$ ,  $j_l$  is the spherical Bessel function of the first kind of order  $l$ ,  $P_l(\cos \Psi)$  is the classical spherical orthogonal Legendre polynomial,  $q_m = |\vec{q}_m| = |\vec{k} - \vec{k}_m| = (\omega/c)(1 + \beta_m^2 - 2\beta_m \cos \theta_m)^{1/2}$ ,  $\beta_m = \omega_m/\omega$ ,  $\theta_m$  is the scattering angle [the angle between wave-vectors of the incident ( $\vec{k}$ ) and scattered ( $\vec{k}_m$ ) photons], and  $\Psi$  is the angle between vectors  $\vec{q}_1$  and  $\vec{q}_2$ . When  $\eta_m \rightarrow 0$ , the imaginary term  $i\gamma_{1s}$  ( $\gamma_{1s} = \Gamma_{1s}/2$ ,  $\Gamma_{1s}$  is the natural linewidth of the  $1s$ -vacancy decay) is defined in the energy denominators of (6):

$$\eta_m^{-1} \rightarrow (\eta_m + i\gamma_{1s})^{-1} = P_m - i\pi L_m, \quad (8)$$

$$P_m = \eta_m \Delta_m^{-1}, \quad L_m = (\gamma_{1s}/\pi) \Delta_m^{-1}, \quad (9)$$

where  $\Delta_m = \eta_m^2 + \gamma_{1s}^2$ . Transformation (8) removes the corresponding singularities in the  $D$  function.

Let us find the triple differential cross section of process (1) over states  $X_1$  and  $X_2$ . Consider the case of coplanar (vectors  $\vec{k}$ ,  $\vec{k}_1$ , and  $\vec{k}_2$  are in the same plane) and symmetric ( $\theta_1 = -\theta_2 \equiv \theta$ ) scattering of linearly polarized (perpendicular to the scattering plane,  $\perp$ ), incident (parallel to each other), and scattered photons:  $(\vec{e} \parallel \vec{e}_m) \perp P$ ,  $(\vec{e} \cdot \vec{e}_m) = \pm 1$ . Here,  $P$  is the scattering plane, defined by vectors  $\vec{k}$  and  $\vec{k}_m$ . In other words, we propose an experimental scheme where detectors for the scattered photons are placed in the scattering plane symmetrically relative to the axis of propagation of the incident XFEL radiation. Transition to the construction of the noncoplanar and asymmetrical Rayleigh scattering cross section and, as a result, the general picture of angular and energetic distribution of the scattered photons is a subject of future investigations. Taking into account Fermi's golden rule

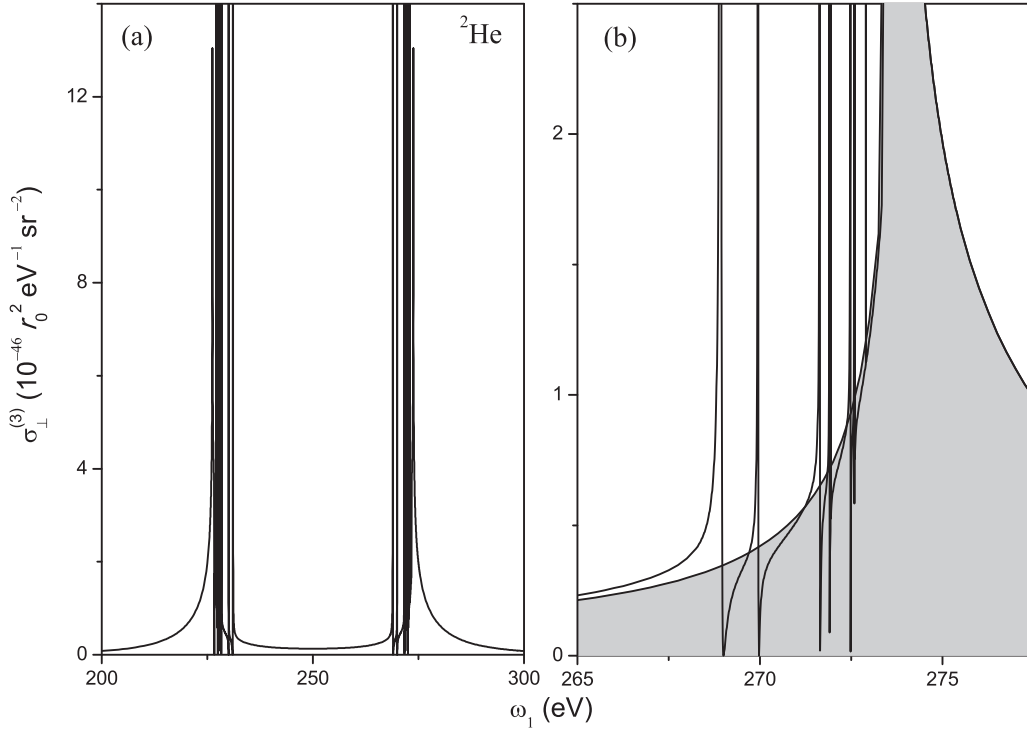


FIG. 2. Triple differential cross section for the Rayleigh scattering of two linearly polarized (perpendicular to the scattering plane,  $\perp$ ) XFEL photons by a He atom. (a) full scattering spectrum with  $\omega = 250$  eV and  $\theta = 90^\circ$ ; (b) part of the full scattering spectrum resolving the structure of the  $1s \rightarrow nl$  excitation resonances accounted for in this work. Shaded part of the spectrum in (b) is the contribution of  $1sx/l$  continuous spectrum states before taking into account the interference of their amplitudes with the amplitudes of the discrete spectrum states.  $\omega(\omega_1)$  is the incident (scattered) photon energy,  $\theta$  is the scattering angle. Spectral characteristics of the leading scattering resonances are given in Table II.

(Fermi [3]):

$$d^4\sigma_{\perp} = \frac{2\pi}{J} |\Phi|^2 \delta(2\omega - \omega_1 - \omega_2) d^2f_1 d^2f_2. \quad (10)$$

Here,  $J = cn/V$  is the density of flux of incident XFEL photons (in our case,  $n = 2$ ),  $d^2f_m = V(2\pi c)^{-3} \omega_m^2 d\omega_m d\Omega_m$ , and  $\Omega_m$  is solid angle of the outgoing scattered photon. Then, integrating (10) over  $\omega_2$  and fixing the quantization volume  $V(\text{cm}^3) = c$  [6], we obtain:

$$\frac{d^3\sigma_{\perp}}{d\omega_1 d\Omega_1 d\Omega_2} \equiv \sigma_{\perp}^{(3)} = \frac{c}{128\pi} r_0^4 \beta_1 (2 - \beta_1) |D|^2, \quad (11)$$

where  $r_0$  is the classical electron radius. From (11) with  $\omega_1 \rightarrow 0$  ( $\omega_2 \rightarrow 2\omega$ ) it follows that  $\sigma_{\perp}^{(3)} \rightarrow 0$ . This result may be interpreted as follows. In the investigated Rayleigh scattering process, confluence of two XFEL photons into one scattered photon with the disappearance of the other one cannot occur.

### III. RESULTS AND DISCUSSION

Results of the calculation of triple differential scattering cross section (11) for the scheme assumed here are shown on Fig. 2 and Tables I, II, and they show the following. As expected, with the largest probability, the energy of the incident XFEL photons is redistributed into two regions of energies for the scattered photons [Fig. 2(a)]:  $\omega_1 \sim \omega \pm I_{1s}$ . Indeed, at time  $t_1$  [see, for example, Fig. 1(a)], one of the incident photons gives up a part ( $\sim I_{1s}$ ) of its energy for the excitation (ionization) of the atom, and leaves the contact interaction

region as a scattered photon of frequency  $\omega_2 < \omega$ . The other incident photon at time  $t_2 > t_1$  receives energy of the excitation (ionization) of the atom, and leaves the contact interaction region with the frequency  $\omega_1 > \omega$ . From a mathematical standpoint, the largest contribution to the improper integrals over  $x$  in (6) comes from the neighborhood of the pole  $x \approx 0 \Rightarrow \omega_1 \approx \omega \pm I_{1s}$ . Moreover, this contribution has a stark resonant character over the continuous spectrum of virtual states of  $1s \rightarrow xl$  scattering (Fig. 2). According to Table I,

TABLE I. Energetic and angular dependence of the triple differential Rayleigh scattering cross section of two XFEL photons by a He atom for the leading giant resonance of the monopole  $1s \rightarrow 2s$  excitation  $\{\omega_1 = \omega \pm [E(1s2s) - E(0)]\}$ ,  $\gamma_{1s} = 1.69 \times 10^{-14}$  eV.  $\omega(\omega_1)$  is the energy of the incident (scattered) photon,  $\theta$  is the scattering angle. The symbol  $[-n]$  denotes a multiplicative factor of  $10^{-n}$ .

$\omega$ (eV)	$\theta$ (degree)	$\sigma_{\perp}^{(3)} (r_0^2 eV^{-1} sr^{-2})$
250		1.275 [-27]
500	90	0.862 [-27]
750		0.425 [-27]
	0	1.443 [-27]
	45	1.392 [-27]
250	90	1.275 [-27]
	135	1.166 [-27]
	180	1.123 [-27]

TABLE II. Spectral characteristics of the leading resonances of the Rayleigh scattering spectrum of two XFEL photons by a He atom with  $\omega = 250$  eV and  $\theta = 90^\circ$  [see Fig. 2(b)].  $\omega_1 = \omega + E(1snl) - E(0)$ ,  $\gamma_{1s} = 1.69 \times 10^{-14}$  eV for the metastable  $1s(ns, nd, nf)$  states and  $\gamma_{1s} = 5 \times 10^{-8}$  eV for the dipole-broadened  $1snp$  states.

$nl$	$\omega_1$ (eV)	$\sigma_{\perp}^{(3)}(r_0^2 eV^{-1} sr^{-2})$
$2s$	268.93	1.275 [−27]
$3s$	271.64	2.013 [−30]
$4s$	272.48	0.620 [−33]
$2p$	269.95	1.652 [−36]
$3p$	271.90	0.918 [−37]
$4p$	272.58	1.383 [−38]
$3d$	271.94	1.898 [−37]
$4d$	272.64	0.221 [−38]
$5d$	272.90	1.093 [−39]
$4f$	272.60	1.126 [−45]
$5f$	272.90	1.337 [−46]
$6f$	273.07	1.313 [−46]

the scattered XFEL radiation is concentrated with the largest probability in the region of  $\theta \approx 0^\circ$  (forward scattering).

According to Fig. 2, scattering probability happens to be nonzero and without redistribution of energy of the incident XFEL photons. This result may be interpreted as the effect of Thomson scattering. Indeed, for the case of scattering of one photon by an atom, Thomson scattering in the nonrelativistic form-factor approximation for the  $f$  amplitude of the scattering probability (Kissel *et al.* (1980) [2]);  $f = \sum_{nl \leq F} N_{nl} \langle nl | j_0(qr) | nl \rangle$ ,  $q = (2\omega/c) \sin(\theta/2)$  ( $N_{nl}$  is the filling number for the  $nl$  atomic shell) can be thought of as the elastic contact scattering of the photon by atomic electron shells without virtual excitation (ionization) of the atom. In other words, the energy of the incident photon is not transferred into an excitation (ionization) of the atomic electron shells. Simultaneously, an exclusively quantum effect is realized—spontaneous creation (annihilation) of a virtual  $(1s, xl)$  pair for the  $1s \rightarrow xl$  ionization state at the contact interaction vertices and with scattered photon energies  $\omega_1 = \omega_2 = \omega$  [see  $D = 2 \sum_{x>F} Q \eta^{-1}$ ,  $\eta = E(0) - E(1sxl) < 0$ ]. Therefore, the Rayleigh scattering of two XFEL photons by an atom is commensurate with the process where the incident photon energy is not spent on the creation of the  $(1s, xl)$  pair. According to the uncertainty principle  $\Delta t \cdot \Delta E \geq \hbar$  [3], we obtain an estimate of the timescale over which the conservation of energy is violated for the virtual level: with  $\Delta E \cong m_e c^2$  (rest energy for the  $xl$  electron) we have  $\Delta t \geq 10^{-21}$  s. Thus, in the studied process (1), Thomson scattering is a special case of Rayleigh scattering.

The leading structures in the scattering spectrum are giant ( $\sigma_{\perp}^{(3)} \sim 10^{-27}$  in Tables I, II, and  $\sim 10^{-46}$  on Fig. 2) scattering resonances defined by Cauchy-Lorentz functions  $L_m$  in (8). An analogous theoretical result, but for the case of Rayleigh scattering of one photon by a He atom, was obtained in Ref. [7]. Large differences in the order of magnitude of cross sections of scattering via discrete and continuous spectra arise from the long lifetimes of the  $1s$  vacancy of  $1sxl$  excitation (ionization) states of He. Thus, according to the

theoretical result of Ref. [8], the lifetime of the metastable  $1s2s(^1S_0)$  state is  $\tau = 19.5$  ms. In this work, we take  $\gamma_{1s} = (1/2) \tau^{-1} = 1.69 \times 10^{-14}$  eV for the metastable  $1snl$  ( $l \neq 1$ ) excited states,  $\gamma_{1s} = 5 \times 10^{-8}$  eV (estimate from theoretical work of Ref. [9]) for the dipole-broadened  $1snp$  excited states; from the complete set of states of the discrete spectrum, we limit ourselves by considering  $1sns$  ( $n = 2, 3, 4$ ),  $1snp$  ( $n = 2, 3, 4$ ),  $1snd$  ( $n = 3, 4, 5$ ), and  $1snf$  ( $n = 4, 5, 6$ ) states.

For the continuous spectrum states we took  $\gamma_{1s} = 5 \times 10^{-8}$  eV, and limited ourselves to the consideration of the quantum numbers  $l \in [0; 17]$ . Taking into account  $l \geq 18$  changes the magnitude of the cross section (11) by no more than 0.1%. While calculating integrals  $R_l^{(m)}$  in (7) within the single-configuration Hartree-Fock approximation through methods of the nonorthogonal orbitals theory [10], we included the effect of radial relaxation [4] of the  $1sxl$  atomic excited (ionized) state wave functions:

$$R_l^{(m)} \rightarrow \langle 1s_0 | 1s_+ \rangle \langle 1s_0 | j_l(qmr) | xl_+ \rangle. \quad (12)$$

This effect is characterized by the destruction of the  $1s^2$  screen between the atomic nucleus and the  $xl$  electronic states above the Fermi level. As a result, a decrease in the average radius of the  $1s_+$  electron of the atomic core, and an additional delocalization of the radial part of the  $xl_+$  wave function occurs. In (12), the radial part of the  $1s_0$ -electron wave function is obtained by solving the Hartree-Fock nonlinear integral-differential equation for the self-consistent field for the ground-state atomic configuration [0]. Radial parts of wave functions of  $1s_+$  and  $xl_+$  electrons are obtained by solving Hartree-Fock equations for the  $1s_+xl_+(T)$  (in the field of the  $1s$  vacancy) configurations of the excited (ionized) atomic state.

In particular, according to (12) and (B21), because of the radial relaxation effect the probability of forward Thomson scattering does not become zero:  $R_0^{(m)} = \langle 1s_0 | 1s_+ \rangle \langle 1s_0 | xs_+ \rangle$ ,  $R_{l>0}^{(m)} = 0$ . Thus, we establish a very important role of the radial relaxation in determining the nonzero probability of Rayleigh scattering of two XFEL photons by an atom. At  $\theta = 90^\circ$  for Thomson scattering [see Fig. 2(a) with  $\omega_1 = \omega$ ] we obtain from (B13)  $\cos \Psi = 0 \Rightarrow P_l(0) = 0, l = 2n + 1; (-1/4)^n C_{2n}^n, l = 2n, n \geq 0$ . Therefore, in contrast to the forward scattering, an infinite set of even Bessel functions contributes to the Thomson scattering probability at  $\theta = 90^\circ$ . As a result, the interference of orbital  $l$  symmetries, and the energetic dependency in (6) define the angular anisotropy effect (see Table I) for the Rayleigh scattering of two XFEL photons by an atom.

According to Fig. 2(b), scattering resonances are buried within the scattering spectrum structures, which replicate the form of Fano autoionization profiles [11] for the angular anisotropy parameter in the He double photoexcitation cross section ([12] and references therein). However, Rayleigh scattering of two photons by an atom shows a different physical mechanism for the appearance of such structures. In particular, these structures are not due to the electrostatic mixing between the continuous spectrum wave functions and the autoionization states buried in them. These structures appear because of the interference in (6) of the probability amplitudes of scattering through ionization states with the real parts [see function  $P_m$

in (8)] of the probability amplitudes of scattering through excitation states.

In concluding this section, let us note the following. The process under investigation can be physically interpreted as a process of photon-photon scattering [via virtual excitation (ionization) of the atom]. Within the framework of quantum electrodynamics, the attempt for theoretical description of photon-photon scattering (via virtual excitations of the electron-positron vacuum) has led to the discovery of corrections (nonlinear in the electromagnetic field) to the classical electrodynamics Lagrangian (see Ref. [13] and references therein). There is interest in setting up the problem of searching for similar corrections that rely on the atomic nature of the medium through which laser radiation is propagating. Full photon-photon scattering cross section via quantum electrodynamics vacuum even for relativistic photon energies ( $\approx 1$  MeV) constitutes a small (and so far not experimentally measured) value  $\sim 3 \times 10^{-30}$  cm<sup>2</sup> [14]. However, for the case of photon-photon scattering via an atomic medium the process cross section might be quite observable (given the expected brightness of XFEL radiation [1]) even for nonrelativistic XFEL-photon energies. For example, for  $N \approx 10^{26}$  photons in the x-ray pulse, the observable triply differential Rayleigh scattering cross section with  $\omega = 250$  eV,  $\omega_1 = 268.93$  eV, and  $\theta = 90^\circ$  (see Tables I and II), due to the theorem of addition of probabilities of disjoint events [15], takes a quite measurable value of  $C_N^2 \sigma_\perp^{(3)} \approx 0.5$  (cm<sup>2</sup> eV<sup>-1</sup> sr<sup>-2</sup>).

#### IV. CONCLUSIONS

We formulated a nonrelativistic quantum theory for the process of Rayleigh (elastic) scattering of two XFEL photons by a free atom. With the He atom as an example, we obtain the absolute values and the forms of the triple differential scattering cross section. For the suggested experimental scheme we find that (i) with largest probability, the incident photon energy is redistributed into two starkly highlighted regions for the scattered photons  $\omega_1 \sim \omega \pm I_{1s}$  and (ii) the leading structures in the spectrum are the giant scattering resonances due to virtual excitations of the atom into discrete spectrum states. At the same time, the cross section does not become zero even for photons with  $\omega_{1,2} = \omega$  (Thomson scattering). Thus, Rayleigh scattering of two XFEL photons by a free atom is accompanied by a quantum effect of spontaneous creation (annihilation) of virtual ionization states of the atom. We also establish the effect angular anisotropy of the Rayleigh scattering—the scattering probability increases as the scattering angle decreases.

The obtained results are important, first of all, for the case of scattering of two XFEL photons by a many-electron atom (multicharge positive atomic ion) with large values of  $I_{nl}$  energies of ionization thresholds for deep and intermediate  $nl$  shells. We note here that for many-electron atoms (or atomic ions) in (6) there is an additional summation (quantum interference of the scattering probability amplitudes) over all of the  $nl \leq F$  core shells. The corresponding analytical representations for the  $Q$  function can be obtained by the methods of Appendix B, and are not given in this paper. In this case, hot photons with energy  $\omega_1 \in (\omega + I_{nl}; 2\omega)$  will be created within the Rayleigh scattering process. Therefore,

a many-electron atom (multicharge positive atomic ion) can significantly increase the energy of the incident XFEL photon. This statement assumes that  $2\omega \gg I_{nl}$  (see Sec. II). Lifting this restriction by accounting for partial probability amplitudes in Figs. 1(c) and 1(d), going outside of the Hartree-Fock single-configuration approximation framework, and taking into account the transition probability amplitudes while including operator (4) and the completeness of the intermediate scattering  $xl$  states are all subject of future investigations. Also of interest is the generalization of this work's results for the processes of Rayleigh scattering of  $n$  ( $n \geq 1$ ) XFEL photons by a free atom (atomic ion) with the creation of  $m$  ( $m \geq 1$ ) scattered photons. It should be expected that in this case too, the small scattering cross section of a single atom (atomic ion) will be compensated by a large binomial factor in the observed differential scattering cross section  $C_N^n \sigma^{(2m-1)}$ . Of course, Furry and Landau-Yang theorems [16] dictate that  $n + m = 2g$ , where  $g$  is a positive integer ( $g \geq 1$ ).

#### ACKNOWLEDGMENT

The authors are grateful to the referees for valuable remarks.

#### APPENDIX A

The total probability amplitude for process (1) in the second order of quantum mechanical perturbation theory over the interfering scattering states  $X_1$  and  $X_2$  [see Figs. 1(a) and 1(b)] has the following form in the Dirac notation:

$$\Phi_{ij} \equiv \Phi = \sum_m \sum_{x>F} \sum_{MT} \frac{W_{ix}^{(m)} W_{xj}^{(m)}}{E_i - E(X_m)}, \quad (\text{A1})$$

$$W_{ix}^{(m)} = \langle i | \hat{W} | X_m \rangle. \quad (\text{A2})$$

Here, we define the full wave functions of the initial  $|i\rangle = |0; \omega\omega\rangle$ , intermediate  $|X_m\rangle = |1sxl(MT); \omega\omega_m\rangle$ , and final  $|j\rangle = |0; \omega_1\omega_2\rangle$  scattering states,  $E$  is full Hartree-Fock scattering state energies,  $T = LSJ$  is a term, and  $M$  is a projection of the full angular momentum  $J$  of the excitation (ionization) state of the atom. Taking into account the structure of the contact transition operator (3), the expression for  $\hat{A}$  operator of the electromagnetic field in the second quantization representation [17], and the factoring of full wave functions of the scattering state into a product of atomic and photon components, we obtain (5) from (A1) and (A2).

Here we note three things. First. The infinite sum over the states of the discrete spectrum in (A1) is replaced by a finite sum. Thus, the requirement of completeness of the set [3] of virtual states of excitation and ionization of the atom is violated. Moreover, together with the neglecting of operator (4), the loss of completeness violates local gauge invariance of the scattering cross section (11). An example of an analytic solution for the problem of building such a set is given in a recent paper [18] (the concept of an expanded infinite-dimensional Hilbert space). However, the problem of accounting for such a set in (A1) remains open. As a result, in (A1) we conducted direct summation (integration) over the  $xl$  states taking into account the finite number of the discrete spectrum states only (see Table II). An alternative to direct summation (integration) is the method of correlation

functions used, for example, in the relativistic theory of Rayleigh scattering of a photon by an atom (Kane *et al.* [2]). In this method, the problem of the construction and direct summation (integration) for the full set of  $xl$ -states does not occur. However, in the nonrelativistic Hartree-Fock single configuration approximation for wave functions of electron states and the x-ray energy photons incident on the atom, it is problematic to solve the integral-differential equations for an infinite [ $l \in [0; \infty)$ ] set of correlation functions. This problem also remains open. Second. The region of integration over the states of the continuous spectrum is represented by the union of regions  $A_N$  and  $B_N = [x_{2N+1}; \infty)$ . The region  $A_N$ , in turn, is represented by the joining of subdomains  $\Delta_i = [x_{2i-1}, x_{2i}, x_{2i+1}]$ , where  $i = 1, 2, \dots, N$ ,  $x_1 = 0, x_{2N+1} \gg I_{1s}$ . In each subdomain  $\Delta_i$ , a parabolic interpolation of the numerator in (A1) is assumed. In region  $B_N$ , an asymptotic behavior of the form  $(a_N x + b_N)^2 x^{-4}$  is adopted for the numerator of the fraction in (A1), where  $a_N, b_N$  are the parameters of the splicing (Hopersky and Yavna [2], and references therein). During the summation over the states of the discrete spectrum and the analytical integration of the states of the continuous spectrum in the singular areas for the scattered photon energies  $\omega_1 \in (0; \omega - I_{1s2s})$  ( $I_{1s2s} = E(1s2s) - E(0)$ ) and  $\omega_1 \in [\omega + I_{1s2s}; 2\omega)$ , the energy denominators in (A1) are modified by transformation (8). The types of integrals emerging in this case are expressed in terms of elementary functions [19]. Third. The cross section  $1s \rightarrow xp$  [the dipole approximation for operator (4)] of the He atom photoionization in the single-configuration Hartree-Fock approximation with, for example, the energy of the absorbed photon being 100 eV, is equal to 0.304 Mb [20] and is significantly ( $\sim 23\%$ ) different from the experimental value of  $0.393 \pm 0.012$  Mb [21]. This fact (see also Refs. [12,22] and references therein) indicates the need for a treatment beyond the one-electron approximation [4] in the description of wave functions of the transition states in (A1), as well as for accounting of nondipole effects involving operator (4) in the third (and higher) order of the perturbation theory for the process probability amplitude (1). Of course, the difference between the theory and the experimental results cannot serve as a reliable measure of the accuracy of the nonrelativistic Hartree-Fock calculations of this work. Such an evaluation occurs only after obtaining the solution to the problem (referred to in Sec. II) of restoring the local gauge invariance for the cross section (11) and taking into account the [important, especially for light atoms] configuration interaction effects (Jucys [22]) in the description of the wave functions of the atomic states.

### APPENDIX B

According to (A1), the  $Q$  function has the following form:

$$Q = \sum_{TM} \langle 0|L_1^+|TM\rangle \langle 0|L_2^-|TM\rangle, \quad (\text{B1})$$

$$L_m^\pm = \sum_{n=1}^N \exp\{\pm i(\vec{q}_m \cdot \vec{r}_n)\}, \quad (\text{B2})$$

where we define the full wave functions of the initial  $|0\rangle = |0; {}^1S_0(J_0 = M_0 = 0)\rangle$  and intermediate  $|lTM\rangle =$

$|1sxl; TM\rangle$  atomic states, and assume an approximation of the energetic denominator in (A1) being independent of quantum numbers  $MT$ . Let us take into account the following mathematical facts [17].

(i) Expansion of the exponential into a double series over the spherical functions,

$$\exp\{i(\vec{q}_m \cdot \vec{r}_n)\} = \sum_{t=0}^{\infty} i^t [t] j_t(q_m r_n) \sum_{p=-t}^t S_{mn}^{pt}, \quad (\text{B3})$$

$$S_{mn}^{pt} = (-1)^p C_{-p}^{(t)}(\vec{e}_{q_m}) C_p^{(t)}(\vec{e}_n), \quad (\text{B4})$$

where  $\vec{e}_{q_m}$  ( $\vec{e}_n$ ) is the unit vector in the direction of  $\vec{q}_m$  ( $\vec{r}_n$ ),  $r_n = |\vec{r}_n|$  and  $[t] = 2t + 1$ .

(ii) The Wigner-Eckart theorem ( $\delta_{\alpha\beta}$  is the Weierstrass-Kronecker symbol),

$$\langle 0|V_{p,m}^{(t)}|lTM\rangle = (-1)^{J+M} (0||V_m^{(t)}||lT) \frac{\delta_{Jl} \delta_{M,-p}}{\sqrt{[J]}}, \quad (\text{B5})$$

for the matrix element of the  $p$ -multipole contact transition operator:

$$V_{p,m}^{(t)} = \sum_{n=1}^N C_p^{(t)}(\vec{e}_n) j_t(q_m r_n). \quad (\text{B6})$$

(iii) The summation of spherical functions theorem,

$$\sum_{p=-t}^t C_{-p}^{(t)}(\vec{e}_{q_1}) C_{-p}^{(t)*}(\vec{e}_{q_2}) = P_t(\cos \Psi), \quad (\text{B7})$$

$$P_t(\cos \Psi) = \sum_{j=0}^t a_{jt} \cos[(t-2j)\Psi], \quad (\text{B8})$$

$$a_{jt} = \frac{1}{4^t} C_{2j}^j C_{2t-2j}^{t-j}, \quad (\text{B9})$$

$$C_\alpha^\mu = \frac{\alpha!}{\mu!(\alpha-\mu)!}, \quad (\text{B10})$$

$$\cos \Psi = \cos \xi_1 \cos \xi_2 + \sin \xi_1 \sin \xi_2 \cos(\varphi_1 - \varphi_2), \quad (\text{B11})$$

$$\cos \xi_m = \frac{(\vec{k} \cdot \vec{q}_m)}{k q_m}, \quad k = |\vec{k}|, \quad (\text{B12})$$

where the Legendre polynomial is represented as a finite sum (B8) [23] and  $\xi_m \in [0; \pi]$ ,  $\varphi_m \in [0; 2\pi]$  is the spherical angles of vector  $\vec{e}_{q_m}$ . For the case of coplanar and symmetrical scattering (B11) takes the form:

$$\cos \Psi = \frac{1 - (\beta_1 + \beta_2) \cos \theta + \beta_1 \beta_2 \cos(2\theta)}{\sqrt{(1 + \beta_1^2 - 2\beta_1 \cos \theta)(1 + \beta_2^2 - 2\beta_2 \cos \theta)}}. \quad (\text{B13})$$

In particular, with  $\theta = 0^\circ$  and  $180^\circ$  expression (B13) takes the forms of  $\cos \Psi = -1 \Rightarrow P_t(-1) = (-1)^t$  and  $\cos \Psi = 1 \Rightarrow P_t(1) = 1$ , correspondingly.

Then, for (B1) we obtain:

$$Q = P_l(\cos \Psi) \sum_T [J](0 \| V_1^{(J)} \| IT)(0 \| V_2^{(J)} \| IT). \quad (\text{B14})$$

Finally, applying equation (29.5) of Ref. [24] to the reduced matrix element in (B5),

$$(0 \| V_m^{(J)} \| IT) = (-1)^{l-J} \Lambda \sqrt{2[L, J]} (0 \| C^{(J)} \| l) R_J^{(m)}, \quad (\text{B15})$$

$$\Lambda = (s^2(lS) \| s^2(S)s) \left\{ \begin{array}{ccc} 0 & 0 & 0 \\ L & l & J \end{array} \right\} \left\{ \begin{array}{ccc} 0 & 0 & 0 \\ J & L & J \end{array} \right\}, \quad (\text{B16})$$

also taking into account the qualities for the reduced matrix element of the spherical function,

$$(0 \| C^{(J)} \| l) = \delta_{lJ}, \quad (\text{B17})$$

the fractional parentage coefficient,

$$(s^2(lS) \| s^2(S)s) = 1, \quad (\text{B18})$$

and the Wigner  $6j$  symbol,

$$\left\{ \begin{array}{ccc} a & b & 0 \\ d & c & f \end{array} \right\} = (-1)^{a+d-f} \frac{\delta_{ab}\delta_{cd}}{\sqrt{[c, b]}}, \quad (\text{B19})$$

in the standard phase system from (B14) we obtain the  $Q$  function from (7). In (7) for the spherical Bessel function, the following integral Plana-Poisson representation is taken [25]:

$$j_l(x) = \frac{1}{l!} \left(\frac{x}{2}\right)^l \int_0^1 (1-z^2)^l \cos(xz) dz, \quad x \in [0; \infty), \quad (\text{B20})$$

$$j_l(0) = \{1, l = 0; 0, l > 0\}. \quad (\text{B21})$$

- 
- [1] H. Yoneda *et al.*, *Nature (London)* **524**, 446 (2015); K. Tamasaku *et al.*, *Nature Photon.* **8**, 313 (2014); M. Yabashi *et al.*, *J. Phys. B* **46**, 164001 (2013); J. Feldhaus, M. Krikunova, M. Meyer, Th. Möller, R. Moshhammer, A. Rudenko, Th. Tschentscher, and J. Ullrich, *ibid.* **46**, 164002 (2013); C. Bostedt *et al.*, *ibid.* **46**, 164003 (2013); K. Tono *et al.*, *New J. Phys.* **15**, 083035 (2013); H. Fukuzawa, S. K. Son, K. Motomura, S. Mondal, K. Nagaya, S. Wada, X. J. Liu, R. Feifel, T. Tachibana, Y. Ito, M. Kimura, T. Sakai, K. Matsunami, H. Hayashita, J. Kajikawa, P. Johnsson, M. Siano, E. Kukk, B. Rudek, B. Erk, L. Foucar, E. Robert, C. Miron, K. Tono, Y. Inubushi, T. Hatsui, M. Yabashi, M. Yao, R. Santra, and K. Ueda, *Phys. Rev. Lett.* **110**, 173005 (2013).
- [2] L. Kissel, R. H. Pratt, and S. C. Roy, *Phys. Rev. A* **22**, 1970 (1980); P. P. Kane, L. Kissel, R. H. Pratt, and S. C. Roy, *Phys. Rep.* **140**, 75 (1986); L. Kissel, B. Zhou, S. C. Roy, S. K. Sen Gupta, and R. H. Pratt, *Acta Crystallogr. Sec. A* **51**, 271 (1995); J. P. J. Carney and R. H. Pratt, *Phys. Rev. A* **62**, 012705 (2000); R. H. Pratt, *Radiat. Phys. Chem.* **74**, 411 (2005); A. N. Hopersky and V. A. Yavna, *Scattering of Photons by Many-Electron Systems* (Springer-Verlag, Berlin-Heidelberg-New York, 2010); A. Costescu, K. Karim, M. Moldovan, S. Spanulescu, and C. Stoica, *J. Phys. B* **44**, 045204 (2011); A. Surzhykov, V. A. Yerokhin, Th. Stöhlker, and S. Fritzsche, *ibid.* **48**, 144015 (2015); L. Safari, P. Amaro, S. Fritzsche, J. P. Santos, and F. Fratini, *Phys. Rev. A* **85**, 043406 (2012); A. V. Volotka, V. A. Yerokhin, A. Surzhykov, Th. Stöhlker, and S. Fritzsche, *ibid.* **93**, 023418 (2016).
- [3] P. A. M. Dirac, *The Principles of Quantum Mechanics* (Clarendon, Oxford, 1958); E. Fermi, *Notes on Quantum Mechanics* (University of Chicago Press, Chicago, 1960); A. Messiah, *Quantum Mechanics* (Dover, New York, 1999).
- [4] M. Ya. Amusia, *Atomic Photoeffect* (Plenum, New York, 1990).
- [5] S. A. Novikov and A. N. Hopersky, *J. Phys. B* **44**, 235001 (2011); A. V. Korol, *ibid.* **27**, L103 (1994); Th. Mercouris, Y. Komninos, S. Dionissopoulou, and C. A. Nicolaides, *Phys. Rev. A* **50**, 4109 (1994); V. Véniard and B. Piraux, *ibid.* **41**, 4019 (1990); J. L. Madajczyk and M. Trippenbach, *J. Phys. A* **22**, 2369 (1989).
- [6] N. Bloembergen, *Nonlinear Optics* (W. A. Benjamin, New York, 1965).
- [7] Th. Groszges, B. Piraux, and R. Shakeshaft, *Phys. Rev. A* **59**, 3088 (1999).
- [8] G. W. F. Drake, G. A. Victor, and A. Dalgarno, *Phys. Rev.* **180**, 25 (1969).
- [9] O. Keski-Rahkonen and M. O. Krause, *At. Data Nucl. Data Tables* **14**, 139 (1974).
- [10] P.-O. Löwdin, *Phys. Rev.* **97**, 1474 (1955); T. Åberg, *ibid.* **156**, 35 (1967); A. P. Jucys, E. P. Našlenas, and P. S. Žvirblis, *Int. J. Quantum Chem.* **6**, 465 (1972).
- [11] U. Fano, *Phys. Rev.* **124**, 1866 (1961); F. H. Mies, *ibid.* **175**, 164 (1968); B. W. Shore, *Rev. Mod. Phys.* **39**, 439 (1967); U. Fano and J. W. Cooper, *ibid.* **40**, 441 (1968); Ph. Durand and I. Păidarova, *J. Phys. B* **35**, 469 (2002); A. Zielinski, V. P. Majety, S. Nagele, R. Pazourek, J. Burgdörfer, and A. Scrinzi, *Phys. Rev. Lett.* **115**, 243001 (2015).
- [12] L. Argenti, R. Pazourek, J. Feist, S. Nagele, M. Liertz, E. Persson, J. Burgdörfer, and E. Lindroth, *Phys. Rev. A* **87**, 053405 (2013).
- [13] R. Karplus and M. Neuman, *Phys. Rev.* **80**, 380 (1950).
- [14] R. Karplus and M. Neuman, *Phys. Rev.* **83**, 776 (1951); B. De Tollis, *Nuovo Cimento* **32**, 757 (1964); V. B. Berestetskii, E. M. Lifshitz, and L. P. Pitaevskii, *Quantum Electrodynamics* (Butterworth-Heinemann, Oxford, 1999).
- [15] W. Feller, *An Introduction to Probability Theory and its Applications* (Wiley, New York, 1970), Vol 1; D. J. Hudson, *Statistics. Lectures on Elementary Statistics and Probability* (CERN, Geneva, 1964).
- [16] W. H. Furry, *Phys. Rev.* **51**, 125 (1937); C. N. Yang, *ibid.* **77**, 242 (1950); L. D. Landau, *Dokl. Akad. Nauk SSSR* **60**, 207 (1948) [in Russian].
- [17] D. A. Varshalovich, A. N. Moskalev, and V. K. Khersonskii, *Quantum Theory of Angular Momentum* (World Scientific, Singapore, 1988); R. Karazija, *Introduction to the Theory of X-Ray and Electronic Spectra of Free Atoms* (Plenum, New York, 1996).
- [18] A. N. Hopersky and A. M. Nadolinsky, *J. Phys. B* **44**, 075001 (2011).

- [19] A. P. Prudnikov, J. A. Brychkov, and O. I. Marichev, *Integrals and Series* (Gordon and Breach Science, Amsterdam, 1986), Vol. 1.
- [20] A. N. Hopersky, A. M. Nadolinsky, and S. A. Novikov, *Phys. Rev. A* **92**, 052709 (2015).
- [21] J. A. P. Samson and W. C. Stolte, *J. Electron Spectrosc. Relat. Phenom.* **123**, 265 (2002); W. F. Chan, G. Cooper, and C. E. Brion, *Phys. Rev. A* **44**, 186 (1991).
- [22] A. P. Jucys, *Adv. Chem. Phys.* **14**, 131 (1969); R. Krivec, M. Ya. Amusia, and V. B. Mandelzweig, *Phys. Rev. A* **62**, 064701 (2000); A. S. Kheifets and I. Bray, *ibid.* **65**, 022708 (2002); T. Surič, E. G. Drukarev, and R. H. Pratt, *ibid.* **67**, 022709 (2003); A. Y. Istomin, A. F. Starace, N. L. Manakov, A. V. Meremianin, A. S. Kheifets, and I. Bray, *J. Phys. B* **39**, L35 (2006); M. Ya. Amusia, E. G. Drukarev, and E. Z. Liverts, *J. Exp. Theor. Phys. Lett.* **96**, 70 (2012); Z. Chen, Y. Zheng, W. Yang, X. Song, J. Xu, L. F. DiMauro, O. Zatsarinny, K. Bartschat, T. Morishita, S. -F. Zhao, and C. D. Lin, *Phys. Rev. A* **92**, 063427 (2015); A. Liu and U. Thumm, *Phys. Rev. Lett.* **115**, 183002 (2015).
- [23] G. Szegő, *Orthogonal Polynomials* (American Mathematical Society, New York, 1959), Vol. 23.
- [24] A. P. Jucys and A. J. Savukynas, *Mathematical Foundations of the Atomic Theory* (Mintis, Vilnius, 1973) [in Russian].
- [25] G. N. Watson, *A Treatise on the Theory of Bessel Functions* (Cambridge University Press, Cambridge, 1965).